DOI:
10.1016/j.bpj.2016.08.009

Document Version
Peer reviewed version

Energetics of Ion Permeation in an Open-Activated TRPV1 Channel

Christian Jorgensen,[a] Simone Furini,[b] and Carmen Domene,[a,c]*

[a] Department of Chemistry, Britannia House, 7 Trinity Street, King's College London, London SE1 1DB, UK

[b] Department of Medical Biotechnologies, University of Siena, viale Mario Bracci 16, I-53100, Siena, Italy

[c] Chemistry Research Laboratory, Mansfield Road, University of Oxford, Oxford OX1 3TA, UK

* Corresponding author: carmen.domene@kcl.ac.uk Tel: +44 - (0) 2078483868

Abstract

Ion channels enable diffusion of ions down physiological concentration gradients. Modulation of ion permeation is crucial for the physiological functioning of cells and misregulation of ion channels is linked to a myriad of channelopathies. The ion permeation mechanism in the Transient Receptor Potential (TRP) ion channel family is currently not understood at an atomistic level. In this paper, a novel simulation strategy for ion permeation, molecular dynamics simulations with bias-exchange metadynamics, has been employed to study and compare monovalent (Na^+, K^+) ion permeation in the open-activated TRP Vanniloid-1 (TRPV1) ion channel. Using ~3 μs of simulation trajectories, atomistic evidence is presented for the non-selective nature of TRPV1. Our analysis shows that solvated monovalent ions permeate through the selectivity filter with comparable energetic barriers via a two-site mechanism. Finally, an intracellular binding site has been confirmed, located between the intracellular gate residues I679 and E684.

Introduction

Transient Receptor Potential (TRP) ion channels constitute a large and diverse protein family, found in yeast and widespread in the animal kingdom (1). The 28 mammalian TRP channels are divided into six main subfamilies: TRPC (canonical), TRPV (vanilloid), TRPM (melastatin), TRPP (polycystin), TRPML (mucolipin), and TRPA (ankyrin). The TRPV subfamily presently comprises six members (TRPV1–6), and they are found in excitable and non-excitable cells playing a critical role in sensory physiology. TRPV channels act at the level of cells (including synaptic activity and secretion of hormones), and they are critical for the sensory apparatus of mammals (touch, hearing, taste, olfaction, vision and thermal sensation) (1, 2). In particular, TRPV1 mediates nociception and contributes to the sensing and interpretation of diverse chemical and thermal stimuli (2). With this plethora of biological functions, it is not surprising that TRP channels are associated with several channelopathies and serve as major pharmacological targets. Consequently, a mechanistic understanding of ion permeation in TRPV channels is essential.

The three-dimensional atomic structures of the vanilloid receptors-1 (TRPV1) (3) and -2 (TRPV2) (4) have been recently elucidated by means of single-particle electron cryo-microscopy. TRPV1 consists of a tetrameric assembly of four subunits, analogous to those of voltage-gated sodium and potassium channels (5, 6). Each subunit consists of six trans-membrane α-helices (S1–S6) and a P-loop helix. The four subunits adopt a cone-shaped arrangement. Segments S5, S6 and the P-loop constitute the central pore of the channel (Figure 1), which is flanked by a voltage-sensor-like domain formed by the S1–S4 segments (3). On the extracellular side, residues G643-D646 constitute the internal walls of the pore. This is the region responsible for selective conduction of ions (selectivity filter). On the intracellular side, below the selectivity filter, the channel opens into a water-filled cavity, which is separated from the intracellular compartment by the channel gate. In one of the experimental structures of TRPV1, this intracellular gate is wide-open, and consequently ions are free to diffuse between the intracellular compartment and the channel cavity. TRPV1, TRPV2, TRPV3 and TRPV4 channels are permeable to both monovalent and divalent cations (2, 7), and display a low

discrimination between them, with the permeability ratio P_{Ca}/P_{Na} ranging from 1 to 10, and a conductance of 35-80 pS (8). TRPV1 is not known to display a clear selectivity preference for Na^+ or K^+ ions.

Molecular Dynamics (MD) simulations have proven to be a powerful technique for mechanistic studies of ion permeation in ion channels (9-11). In a recent study, MD simulations of the open-activated pore domain of TRPV1 in the presence of three cationic species, K^+, Na^+ and Ca^{2+} were described (12). Cation binding sites were identified at the extracellular side of the selectivity filter, and it was proposed that E648 and D646 residues facilitate permeation. Potassium ions diffuse easily in this region, with binding events of K^+ ions to residue D646 on the order of 10^1-10^2 ns. For sodium ions, several binding events to residue D646 with residence times of the order of 10^2 ns were sampled. The residues of the selectivity filter exhibited a high degree of flexibility in MD simulations of TRPV1, and this feature was also depended on the ion species considered. In the presence of K^+ ions, the selectivity filter preserved a symmetric structure, similar to the one observed experimentally. In contrast, the binding of Na^+ ions at the extracellular entrance of the channel, stabilized an asymmetric state of the four subunits contributing to the selectivity filter. In classical MD trajectories of the TRPV1 channel, only a limited number of permeation events per microseconds were observed.

While MD simulations constitute a powerful tool to relate structure and dynamics with function, they are still limited by the problem of sampling or accessible simulation timescales. To simulate slow or rarely occurring processes, and to predict the associated free energy profiles with efficient use of computational resources, biased methods that accelerate the sampling of the phase (conformational) space have been developed. Metadynamics (13, 14), umbrella sampling (15), and ABF (16) are common strategies for the analysis of conduction in ion channels (17). Within these methods, the properties of an N-atom system are explored as a function of a finite number of d-dimensional collective variables $\xi(x)$, where d is a small number and x is the state of the system, assuming that the set of collective variable provides a good coarse-grained description

of the true 6N-dimensional dynamics. These collective variables can be any explicit function of x such as an angle, a distance, a distance projected on an axis, a coordination number etc. In the case of ion conduction, it is common to use as a collective variable the distance projected along the permeation axis of the channel between the ion and the center of mass of a group of atoms from the protein used as a reference. Whenever the mechanism of conduction involves more than one ion, it is necessary to accelerate sampling for all the ions that might participate in conduction events. This requirement to accelerate sampling for multiple ions has two important consequences. First, the number of ions involved in conduction events might be undefined, as it is in the case of the TRPV1 channel analyzed here. Second, the computational cost to explore the configurational space increases exponentially with the number of collective variables, which further complicates the energetic analyses. Bias-exchange metadynamics (18) (BE-meta) is a strategy available to explore a high-dimensional space of collective variables without an exponential computational cost involved, and without the need to define in advance the number of permeating ions. In BE-meta, several replicas of the system are simulated in parallel, making use and taking advantage of highly-parallelized computer architectures and scalable MD codes like GROMACS (19) or NAMD (20). A metadynamics simulation is performed for each replica using a small set of collective variables, typically one or two. In metadynamics, a history-dependent potential that compensates for the underlying free energy surface along the biased collective variable is added to the potential energy of the system. As a consequence, the system is forced to escape local energy minima, and instead explores fully the space of the collective variables. In BE-meta simulations, each replica is biased along different collective variables, with the bias acting on the i-th replica given in terms of the height (w) and width (δ) of the Gaussian for the process described by the collective variable ξ_i:

$$V_i\left(x_i,t\right) = w\sum_{t'<t}\exp\left(-\frac{\left(x_i\left(x_i(t)\right) - x_i\left(x_i(t')\right)\right)^2}{2\delta^2}\right) \qquad \text{Equation (1)}$$

where $x_i(t)$ is the configuration of the system in the i-th replica at time t. At fixed time intervals, an exchange between replicas is attempted taking into account a Monte Carlo acceptance criterion. The atomic coordinates of two randomly selected replicas (x_1 and x_2) are exchanged if replica swapping increases the total biasing potential ΔV:

$$\Delta V = V_1(x_1,t) - V_1(x_2,t) + V_2(x_2,t) - V_2(x_1,t) \qquad \text{Equation (2)}$$

where V_1 and V_2 are the biasing potentials in two replicas, respectively accelerated along the collective variables ξ_1 and ξ_2. In the opposite situation, when the exchange results in a decrease of ΔV, the swap is accepted with a probability equal to exp(βΔV), where β is the inverse temperature. In this way, the dynamics along the biased collective variable(s) of a certain replica is accelerated by the metadynamics biasing potential and swapping configurations between replicas improves sampling along the collective variables biased by the whole set of simulations. Thus, by adopting this strategy, permeation of one ion per replica can be accelerated at the same time as the exploration of the multidimensional configurational landscape defined by the ions accelerated in the other replicas. The Potential of Mean Force (PMF) acting along the collective variable ξ_i is given by:

$$A_i(x_i) = -\frac{1}{\Delta t}\int_{t_{eq}}^{t_{eq}+\Delta t} V_i(x_i,t)\,dt \qquad \text{Equation (3)}$$

where t_{eq} is an equilibration time required to explore the entire space of the collective variable, and Δt is a time interval used to average out the oscillations of the biasing potential. A recent study employed BE-meta simulations to successfully elucidate the thermodynamics of ion permeation in a toy model of a Na^+ selective channel (21). Here, a similar approach is used to obtain PMFs for the permeation of sodium and potassium ions in the TRPV1 channel.

Materials and methods

Atomic model of the TRPV1 selectivity filter

An atomic model of TRPV1 based on the experimental structure of the vanilloid receptor 1 (Protein Data Bank entry 3J5Q) (3) was used. The model included only the region of the selectivity filter, and the surrounding residues (residues F587 to Y671). Based on previous work on TRPV1, an equilibrated snapshot was used from a 200-ns MD trajectory of TRPV1 in the NpT ensemble (12). The system was solvated in a box of ~9,500 water molecules. N- and C-termini were amidated and acetylated respectively. Default protonation states were used for protein residues based on pKa calculations. Sodium ions were added to the system to achieve electrical neutrality. The system was equilibrated by 10,000 steps of energy minimization with the steepest descent algorithm, followed by 0.5 ns of dynamics in the NvT ensemble, and 1.5 ns in the NpT ensemble, with harmonic restraints applied to the heavy atoms of the protein using a force constant equal to 2.19 kcal $mol^{-1}Å^{-2}$. MD simulations were performed with GROMACS version 4.6.5 (19, 22). The CHARMM27 force field with CMAP corrections was used for the protein (23, 24), together with the TIP3P model for water molecules (25). The Lennard Jones parameters for Na^+ and K^+ ions were respectively ε=0.0469 kcal mol^{-1} and Rmin/2=1.36375 Å, and ε =0.0870 kcal mol^{-1} and Rmin/2=1.76375 Å (26). Temperature was set to 303.15 K, and controlled by velocity rescaling with stochastic terms with coupling time constant set to 0.1 ps (27). A pressure of 1 bar was imposed by coupling to a Parinello-Rahman barostat with coupling time constant of 2 ps (28). Electrostatic interactions were calculated with the Particle Mesh Ewald algorithm (29), with a maximum grid spacing for the Fourier transform of 1.2 Å. Van der Waals interactions were truncated at 12 Å. Bond lengths were restrained with the LINCS algorithm (30). The leap-frog algorithm was used to integrate the equations of motion using a time step of 2 fs.

Atomic model of the TRPV1 pore domain

The model of the pore domain included residues 570–686 (Protein Data Bank entry 3J5Q) (3). The setup was done with CHARMM-GUI (http://www.charmm-gui. org) (31), with the N-terminus being acetylated and an N-methylamide group added to the C-terminus. Default ionization states were used for protein residues. The channel was embedded in a pre-equilibrated lipid bilayer of 153 POPC molecules (1-palmitoyl,2-oleoyl-sn-glycero-3-phosphocholine) using the replacement method of CHARMM-GUI, with the axis aligned to the bilayer normal. Ions were added to neutralize the system and obtain a total ionic background concentration of 150 mM. Equilibration of the full TRPV1 pore was undertaken using 5,000 steps of steepest-descent minimization, 75 ps of dynamics in the NvT ensemble with restraints on the backbone atoms with a timestep of 1 fs, followed by 300 ps of dynamics in the NvT ensemble with restraints on the backbone atoms with a timestep of 2 fs, and finally 1.0 ns of dynamics in the NpT ensemble. This output was used as the starting point for subsequent BE-meta simulations. MD simulations for the full TRPV pore embedded in a POPC lipid bilayer were performed using the same protocol described earlier for the model of the selectivity filter.

Bias-exchange metadynamics simulations

BE-meta simulations of ion conduction in TRPV1 were performed with Plumed (version 2.1.0) (32, 33) and GROMACS (version 4.6.5) (19, 22) using different number of replicas. The number of replicas was set equal to the maximum number of permeating ions considered in a simulation, plus a ‘neutral’ replica. The neutral replica is a simulation that it is not affected by any time-dependent biasing potential but that swaps configurations with the other replicas. Sampling in the neutral replica approximates the equilibrium distribution with an accuracy that improves with slow-changing biasing potentials. The remaining replicas are biased using a time-dependent metadynamics potential that acts on a 1-dimensional collective variable. In this study, the collective variable is defined as the distance along the channel-axis (z-axis) between an ion (a different one in each replica) and the centre of mass of the carbonyl oxygen atoms of

residues G643 that are located at the intracellular entrance of the selectivity filter. In order to control the number of ions inside the channel, the distance between the ion and the channel axis was restricted by half-harmonic potentials. . The distance from the channel-axis was measured as the distance in the xy-plane between the ion and the center of mass of the carbonyl oxygen atoms of residues G643 and M644. The half-harmonic potential was set to zero when this distance was lower than 8 Å, and it was increased using a force constant of 2.19 kcal $mol^{-1}Å^{-2}$ above this threshold, for all the ions biased by metadynamics potentials in any of the replicas. The remaining ions in the systems were excluded from permeation events by applying half-harmonic potentials equal to zero when the distance of the ion from the axis was higher than 8 Å, and increased harmonically inward. Under these conditions, only ions accelerated by the biasing potentials were able to enter the permeation pathway.

A summary of the bias-exchange metadynamics simulation sets is presented in Table 1. Six BE-meta simulations were performed, two of which with the model of the TRPV1 pore domain, using a neutral replica and two replicas with biasing potentials on (i) two K^+ ions (BE_2K_pore) and (ii) two Na^+ ions (BE_2NA_pore). Four BE-meta simulations were performed using the model of the TRPV selectivity filter: (i) a neutral replica and two replicas with biasing potentials acting on the collective variable of two Na^+ ions (BE_2NA), (ii) a neutral replica and two replicas with biasing potentials acting on K^+ ions (BE_2K), (iii) a neutral replica and four replicas with biasing potentials acting on the collective variable of four different Na^+ ions (BE_4NA), and finally (iv) a neutral replica and three replicas with biasing potentials acting on the collective variable of two Na^+ ions, and a K^+ ion (BE_2NA_1K).

A protocol for BE-meta simulations employed on a model of a Na^+ selective ion channel, NavAb, was adapted for this work (21). The collective variable was discretized in bins of 0.5 Å, between -10 Å and +15 Å for the simulations with the model of the selectivity filter, and between -40 Å and +20 Å for the simulations with the model of the pore domain. Gaussians hills with height equal to 6 x 10^{-3} kcal mol^{-1} and width equal to 2.5 x 10^{-3} Å were added to the biasing potential every 2 ps. Exchanges between replicas were

attempted every 50 ps. The biasing potential acted on a different ion in each replica, thus, as the simulation proceeds, the biasing potential of each replica provides an estimate of the PMF experienced by the ion biased in that replica in the presence of the other permeating ions (i.e. the ones accelerated in the other replicas).

Set	**Replicas**	**Replica1**	**Replica2**	**Replica3**	**Replica4**	**t_{eq} (ns)**	**t_{tot} (ns)**
BE_2K	2 biased 1 neutral	K^+	K^+	-	-	50	160 x 3
BE_2NA	2 biased 1 neutral	Na^+	Na^+	-	-	50	110 x 3
BE_4NA	4 biased 1 neutral	Na^+	Na^+	Na^+	Na^+	150	150 x 3
BE_2NA_1K	3 biased 1 neutral	Na^+	Na^+	K^+	-	120	180 x 4
BE_2K_pore	2 biased 1 neutral	K^+	K^+	-	-	80	240 x 3
BE_2NA_pore	2 biased 1 neutral	Na^+	Na^+	-	-	50	240 x 3
					Cumulative simulation time:		**2.94 µs**

Table 1. Summary of bias-exchange metadynamics simulation sets. Two BE-meta simulations with the model of the pore domain, and four BE-meta simulations with the model of the selectivity filter were considered. The ion species accelerated in each replica; the time required for exploring the entire range of the collective variable, from intracellular to extracellular side of the channel, for the entire set of replicas (t_{eq}); and the total simulation time (t_{tot}) are listed.

Results

The selectivity filter of TRPV1 can be divided into two areas: i) the extracellular side denoted SF2, close to the side chain of D646, and ii) the intracellular side denoted SF1, centred at the backbone oxygen atoms of G643 (Figure 1) (12). This disposition is comparable to the architecture of the pore of bacterial Na^+ channels, with an intracellular area lined by carbonyl oxygen atoms, and a ring of negative residues at the extracellular entrance. However, the TRPV1 pore is wider and the sequence is clearly different; GMGD in TRPV1 and TLES in NavAb from *Arcobacter butzleri*.

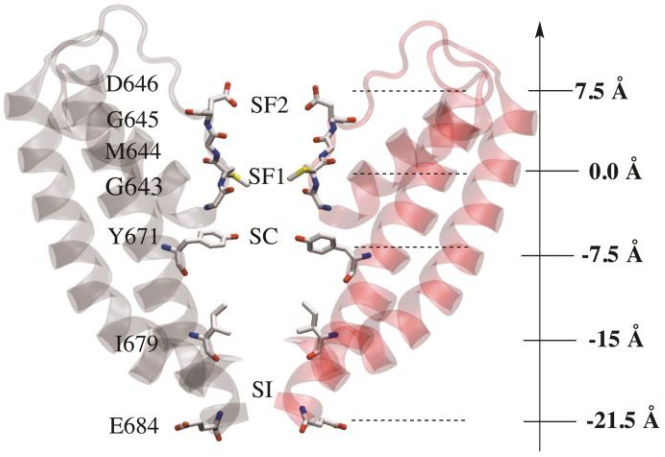

Figure 1. Pore region of the TRPV1 channel. S5, S6 and P-loop helices are shown for two subunits only. Key residues along the ion permeation pathway are labelled and shown in licorice representation. The black arrow at the right side of the structure indicates the collective variable used to accelerate ion movements in bias-exchange metadynamics simulations, i.e. the distance along the permeation pathways (z-axis) with respect to the carbonyl oxygen atoms of G643.

Ion permeation through a model of the selectivity filter of TRPV1

The simulation protocol followed to estimate the energy profile of conduction events was first tested using a simplified model of the TRPV1 channel, which included only the pore residues F587-Y671. The purpose of these simulations was to identify an optimal strategy for the calculation of free energies at a reduced computational cost, and equally, to gain insight into the permeation properties of the selectivity filter of TRPV1 in a highly controlled environment; i.e. the backbone atoms of the residues surrounding the selectivity filter are restrained by harmonic potentials (see Methods section for more details). Subsequently, free energy calculations using the full atomic model of the pore domain of TRPV1 were performed, and they are described in the next section. Since the experimental conductance of TRPV1 is similar for K^+ and Na^+ ions, the PMF for both cations was estimated. Previous MD simulations of TRPV1 suggested that conduction events of K^+ and Na^+ ions involve at least two ions (12). Therefore, the PMF profiles were estimated in the presence of three replicas: a neutral replica, with no biasing potential applied, and two replicas with biasing potential accelerating the movement of an ion along the channel axis (simulations BE_2K and BE_2NA in Table 1). The ions accelerated by biasing potentials are free to move across the channel between the intracellular and the extracellular compartment. In contrast, other ions in the

simulation domain are confined outside the channel. Consequently, simulations BE_2K and BE_2NA describe conduction events with one or two ions involved, e.g. the estimated PMF profile is the energy experienced by an ion in the presence of the second ion. In simulations BE_2K and BE_2NA, the ions accelerated by the biasing potentials explored the entire pore axis (collective variable shown in Figure 1) in less than 50 ns in both replicas (t_{eq} = 50 ns). The time-dependent estimate of the PMF profile in each replica (Equation 3) was used to monitor the convergence of the simulations. Convergence was achieved after 160 ns for K^+ ions and after 110 ns for Na^+ ions (Supp. Mat. Figures S1 and S2). The PMF profile experienced by K^+ ions (Figure 2.a) was estimated as the average of the PMFs calculated for the two replicas (Supp. Mat. Figure S1). Since each replica accelerates permeation of a different K^+ ion, the two simulations provide independent estimates of the PMF experienced by a K^+ ion along the axis of the channel. As K^+ ions are identical, the PMF estimated in two replicas should converge to the same profile. Therefore, the distance between these independent PMF profiles was used as an estimate of the error affecting the energy calculations. The low standard deviation obtained by this procedure (blue bars in Figures 2.a) confirms the convergence of the BE-meta simulation. Identical procedure was used to estimate the average PMF profile and its standard deviation for Na^+ ions as well as for the other ion configurations analyzed (Table 1). The energy profiles estimated for K^+ and Na^+ ions are remarkably similar (Figure 2a,b). In agreement with previous MD simulations of the pore domain (12), two regions attractive for cations are found in the selectivity filter of TRPV1. At the intracellular entrance of the selectivity filter, the energy has a minimum at the carbonyl oxygen atoms of G643 (binding site SF1). At this position, the channel is 9.4 ± 0.4 Å wide, and both K^+ and Na^+ ions bind with the first hydration shell almost intact. Moving outward from SF1, another attractive region for cations is found close to the side chain of residue D646 (binding site SF2). For both K^+ and Na^+, two local energy minima emerge in SF2. In the innermost energy minimum, ions interact with the carbonyl oxygen atoms of residue G645, while at the extracellular entrance of the selectivity filter, ions interact mainly with the side chain oxygen atoms of residue D646. The energy barrier between

the two energy minima characterizing SF2 is minimal (< 1 kcal/mol). Therefore, this region is a unique binding site for cations. In contrast, an energy barrier ~4 kcal/mol separates binding sites SF1 and SF2. It is worth noting that this is the maximum energy barrier for ion movement across the selectivity filter, and that it is comparable with energy barriers estimated for other channels in the conductive state (34-36), suggesting that this model of TRPV1 is permeable to K^+ and Na^+ ions by means of conduction events involving one or two ions. As expected from the electronegative nature of the atoms surrounding the pore (carbonyl oxygen atoms of residues G643 and G645, and side chain of D646), the selectivity filter of TRPV1 is a highly attractive region for cations. The energy difference found between an ion inside the selectivity filter or in the intracellular/extracellular space is 5-6 kcal/mol, which is the highest energy barrier encountered by K^+ and Na^+ ions in a complete conduction event between the intracellular/extracellular compartments, as estimated by simulations with two cations (Figure 2.a,b). The difference in the magnitude of the energy inside and outside the selectivity filter suggests than more than two ions might participate in conduction events across TRPV1. A BE-meta simulation with five replicas was then used to investigate the features of the potential of mean force in the presence of more than two ions inside the selectivity filter (BE_4NA). In this simulation, the movement along the pore axis of four independent Na^+ ions was accelerated, and consequently, the estimated PMF profile corresponds to the energy experienced by a Na^+ ion in the presence of other three Na^+ ions (which could all bind to the selectivity filter at the same time). The difference in energy between the selectivity filter and the outer space disappears when the number of replicas is higher (Figure 2.c, with the convergence of the PMF profile shown in Supp. Mat. Figure S3); this reflects that more than two ions might bind simultaneously in the selectivity filter. The average number of ions inside the selectivity filter in the neutral replica of BE_4NA was 3.1 ± 0.5 (number of ions between ξ = -2.5 Å and ξ = 10 Å). However, the presence of more ions inside the selectivity filter does not alter the binding sites or the energy barriers associated to permeation (compare Figure 2.a with 2.c). This suggests that essential features of the selectivity

filter required for permeation were captured in simulations with two cations, and that permeation events of separate ions across TRPV1 are not correlated. As a further preliminary test of the simulation protocol, if the conduction properties were modified by the presence of K^+/Na^+ ion mixtures was investigated (Figure 2.d). In BE-meta simulations, it is possible to analyze the conduction properties of ion mixtures by accelerating movements of diverse ionic species in different replicas. The set-up of the ion mixture simulation was that of the two sodium-ion simulation, incorporating an additional potassium ion replica, (simulation BE_2NA_1K). Upon convergence after 180 ns (Supp. Mat. Figure S4), both energy profiles for Na^+ and K^+ ions are similar to the ones rendered from simulations with two Na^+ and two K^+ ions respectively, confirming the lack of correlation among the movement of different ions across the selectivity filter.

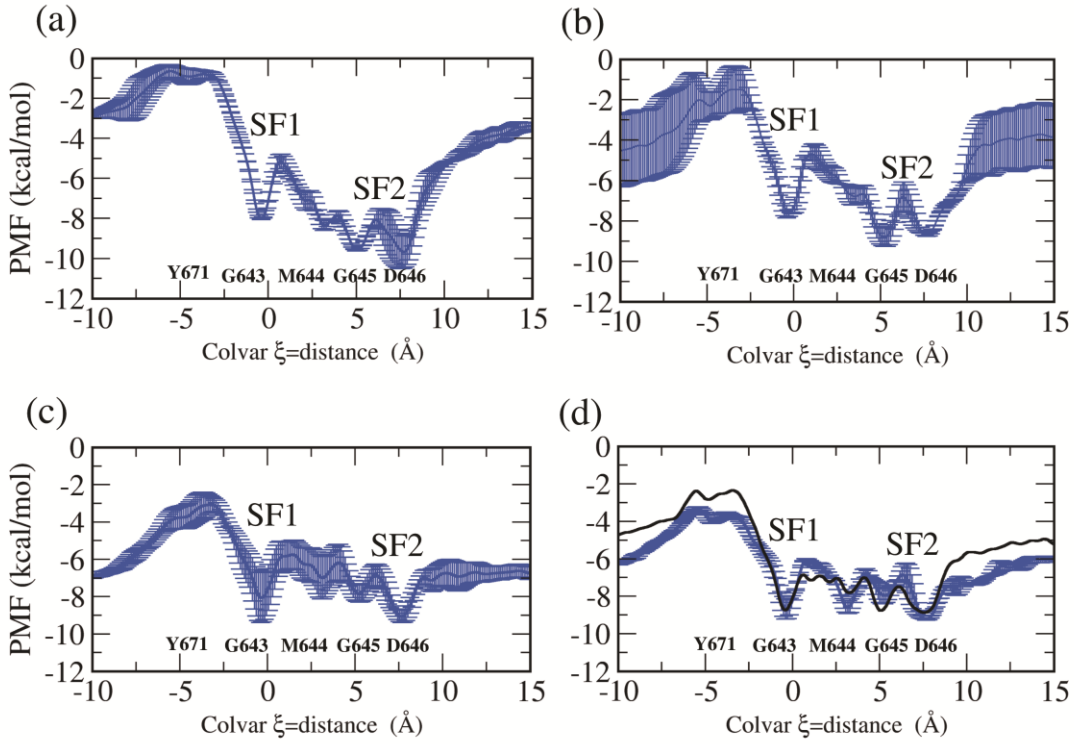

Figure 2. PMF and associated binding sites in a simplified model of TRPV1 estimated in simulations with: (a) two sodium ions (BE_2NA); (b) two potassium ions (BE_2NA), (c) four sodium ions (BE_4NA), and (d) ion mixture of one potassium and two sodium ions (BE_2NA_1K). In the latest case, outputs for sodium and potassium ions are represented in blue and black respectively.

Ion permeation through the pore domain of TRPV1

The simulations with the simplified model of TRPV1 established that tracking two ions suffices to study conduction properties, and that it is possible to analyze permeation of K^+ and Na^+ ions in independent BE-meta simulations. Therefore, BE-meta simulations with two permeating ions, either K^+ or Na^+, were performed using a model of the entire pore domain of TRPV1 (simulations BE_2K_pore and BE_2NA_pore in Table 1). The resulting one-dimensional free energy profile (Figure 3.a, b) corresponds to the PMF experienced by one ion moving across the TRPV1 channel in the presence of the second ion. Convergence is achieved after 200 ns for potassium, and 240 ns for sodium (Supp. Mat. Figure S5 and S6). The energy profiles were similar to the ones estimated with the simplified model of TRPV1, described in the previous section. In particular, analogous binding sites were observed inside the selectivity filter. In the intracellular binding site, SF1, a hydrated K^+ or Na^+ ion aligns with the carbonyl oxygen atoms of residue G643, exactly as observed for the simplified model. A minor difference appears for binding site SF2 where instead of the two local minima previously observed at the extracellular entrance of the channel (Figure 2), a single energy minimum is present in simulations with a model of the entire pore domain (Figure 3.a,b). This difference is likely to reflect a higher degree of mobility of the residues at the extracellular entrance of the channel in simulations with a model of a complete pore domain. However, it is important to remark that the main energy barrier to conduction across the selectivity filter is the transition between SF1 and SF2, in both models of TRPV1. This energy barrier correlates with the constriction of the selectivity filter in the region between residues G643 and G645, and the subsequent decrease in the number of water molecules coordinating the ion. As expected from the wide diameter of the pore, ions navigate through the filter partially solvated. The diameter of the selectivity filer is minimal in the region between residues G643 and G645: 9.3 ± 1.2 Å and 10.4 ± 3.1 Å in potassium and sodium simulations respectively. The energy barrier between SF1 and SF2 is likely to reflect the loss of coordinating water molecules in this region (Supp. Mat. Figure S7). In previous work using conventional classical molecular dynamics (12), it was reported that the

selectivity filter deviates from a symmetric structure and evolves to a dimer of dimers structure in the presence of Na^+ ions but not in the presence of K^+ ions. The same behaviour was observed in simulations BE_2K_pore (Supp. Mat. Figure S8.a,c,e) and BE_2NA_pore (Supp. Mat. Figure S8.b,d,f).

At the intracellular side of binding site SF1, the energy profile is almost flat for the first 15 Å (ξ = -40 Å to -25 Å), which corresponds to the intracellular cavity of the channel. The simplified model of TRPV1 analyzed in the previous section was truncated to the P-loop region of the channel. Consequently, the simplified model could not reproduce correctly the energy profiles in this region. The presence of an intracellular cavity where ions are free to diffuse is a hallmark of several ion channels, including K^+ and Na^+ channels (37). In TRPV1, a fourth binding site for cations was identified at the intracellular side of the channel; I679 is the main constriction residue in the cryo-EM structure of TRPV1,(38) while E684 creates an electronegative potential attractive for cations, similar to D646 at the extracellular entry. Negative residues at the intracellular mouth of the channel are expected to increase the effective concentration of cations entering the pore, with a subsequent effect on the conductance. The effect of negative residues on channel conductance has been proved theoretically and experimentally in BK K^+-channel (39, 40). The low energy of binding site SI suggests that residue E684 might have a similar effect on the conductance of TRPV1.

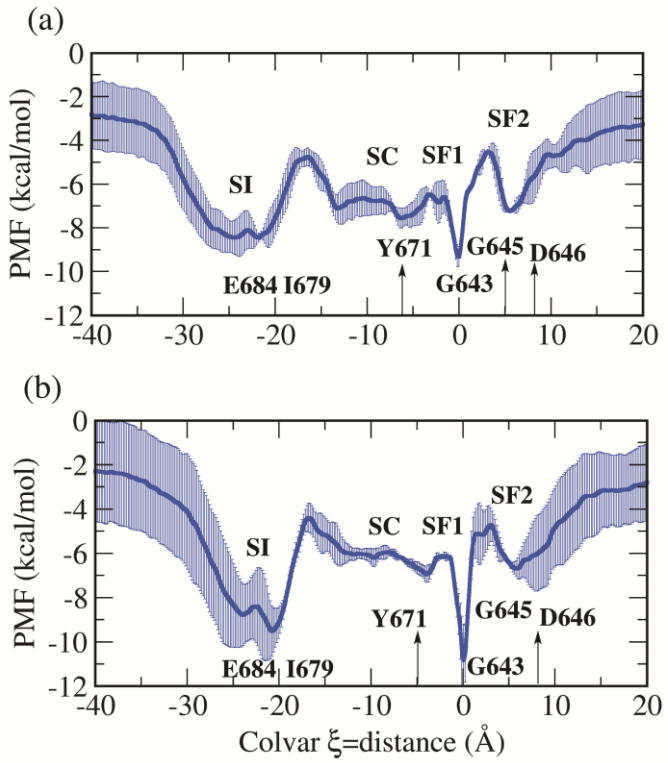

Figure 3. PMF and associated binding sites of (a) K^+ and (b) Na^+ ions in a model of the pore domain of TRPV1 estimated in simulations with two permeating ions (BE_2K_pore and BE_2NA_pore).

Discussion & Conclusions

The recent availability of a structure of TRPV1 from cryo-electron microscopy has made possible to investigate how TRP channels operate at the atomic level using computational methods. In a previous study (12), analyses of ion permeation by classical MD simulations revealed that: i) two attractive regions for cations exist in the selectivity filter of TRPV1, one at the intracellular side (SF1) and one at the extracellular side (SF2); and ii) the selectivity filter is highly flexible. In particular, a structural change of the selectivity filter from a symmetric to an asymmetric structure (C4 vs C2 symmetry) was observed in simulations with Na^+ ions. In the present study, the energetics of ion conduction across TRPV1 was analyzed by BE-meta simulations. The acceleration of ion movements by biasing potentials in BE-meta simulations rendered more efficient sampling of the configurational space than in classical MD simulations, and consequently a more accurate estimate of energy profiles. BE-meta simulations of the

TRPV1 pore confirmed the presence of two binding sites for cations in the selectivity filter: SF1 at residue G643 and SF2 at residue D646. Furthermore, BE-meta simulations revealed that SF1 and SF2 have similar energies and that the transition between SF1 and SF2 corresponds to the highest energy barrier for conduction of Na^+ and K^+ ions across the selectivity filter of the channel. The intracellular cavity (SC) of TRPV1 emerged as a flat-energy region, in agreement with what it is observed in other ion channels (41, 42). In contrast, the free energy profiles reveal an additional binding site at the intracellular entrance of the channel denoted SI, where ions interact with the negatively charged residues E684. Our simulations describe conduction through TRPV1 in terms of diffusion of independent ions across a series of binding sites (SF2/SF1/SI).The low-correlation amid ion movements across the selectivity filter is testified by the high similarity between the energy profiles estimated using either two or four ions, or ion mixtures. This lack of correlation differentiate TRPV1 from K^+-channels, where permeation can be described as the concerted movement of a single file of dehydrated K^+ ions (34, 43, 44), and also from permeation in bacterial Na^+ channels. In bacterial Na^+ channels, ion movements are only weakly correlated, but still permeation was described as a two- or three-ion process (36, 45, 46). In contrast, in TRPV1, permeation is more accurately described as a one-ion process. Indeed, while more than one ion might populate the selectivity filter at any time, the presence of more ions is not required for translocations between SF1 and SF2. Beyond this different conduction mechanism, the main difference between TRPV1 and bacterial Na^+ channels is that TRPV1 is non-selective for monovalent ions. In Na^+ channels, the smaller Na^+ ions are energetically favoured over K^+ ions in the constriction region between the intracellular and the extracellular binding sites. TRPV1 exhibits binding sites of similar architecture to those in bacterial Na^+ channels at the intracellular/extracellular entrance of the filter. However, the selectivity filter of TRPV1 is more flexible than that of NaVAb, rendering a wider diameter at the constriction region (9.6 Å for NavAb at E117-E117 vs 12.8 Å for TRPV1 at G645-G645), which could explain the lack of selectivity between Na^+ and K^+.

The high degree of flexibility monitored for the residues of the selectivity filter in the simulations of TRPV1 is a unique characteristic among the ion channels studied by us using MD simulations. In K^+-channels, the conductive state is characterized by a well-defined structure of the selectivity filter, where minimal deviations from the canonical structure were responsible for significant changes in the energetics of ion conduction (47, 48). Similarly, rotation of a backbone angle of a residue of the selectivity filter in NaK channels was responsible for transitions between a state with low energy barriers for ion permeation, and a state impermeable by cations (49). The residues in the selectivity filter of bacterial Na^+ channels exhibit higher mobility compared to K^+-channels and NaK. In particular, the glutamate residues at the extracellular entrance of NaVAb might switch among different states (50). However, the architecture of the selectivity filter of bacterial Na^+ channels does not deviate from the experimental structure in microseconds trajectories. Instead, deviations from the experimental structure of TRPV1 were observed in sub-microsecond trajectories. The selectivity filter of TRPV1 in the BE-meta simulations is more stable when potassium ions are considered as opposed to sodium ions. In the latest case, the selectivity filter lowers its symmetry, and evolves from C4 to C2 symmetry (Supp. Mat. Figure S8) as reported from classical MD simulations (12). The PMF profiles for permeation events of Na^+ and K^+ ions estimated from BE-meta simulation provided new insights into the functional role of these structural changes of the selectivity filter. The main energetic features were conserved between simulations using a model of the pore domain and those using a simplified model of the channel. In the simplified model, structural changes of the selectivity filter were prevented by harmonic restraints. The conservation of energetic features in the presence of structural changes or with the filter restrained to the experimental structure suggests that ion conduction in TRPV1 is mainly driven by long-range electrostatic forces, and not by intimate atomic interactions with protein atoms.

The work presented here complements the recent simulation work on apo and holo-TRPV1 structures with its capsaicin agonist bound (51), and permeation in TRPV from unbiased MD simulations (12). In conclusion, bias-exchange metadynamics simulations

have been employed to probe the thermodynamics of monovalent ion conduction in the transient receptor potential vanniloid-1 ion channel, using a simplified model and a model of the entire pore domain. Bias-exchange metadynamics is proved to be an efficient strategy for estimating the PMF profile of permeation events, in particular in cases where the number of permeating ions is unknown, or permeation events with different number of ions coexist. It was found that TRPV1 is a non-selective ion channel, with similar monovalent ion permeation profiles for sodium and potassium, displaying barriers of 2-4 kcalmol^{-1} for both ions. Two-ion simulations were sufficient to describe ion conduction across the TRPV1 selectivity filter by a diffusive model where ions translocate between three main binding sites SF2, SF1 and SI. These results pave the way for a promising new approach to study selectivity and permeation in ion channels and in the greater context of TRP channel functioning.

Acknowledgements

C.J. thanks King's College London for a GTA studentship. C.D. acknowledges use of ARCHER, the UK National Supercomputing Service (http://www.archer.ac.uk) and the National Service for Computational Chemistry Software (NSCCS).

References

1. Venkatachalam, K., and C. Montell. 2007. TRP channels. Annual Review of Biochemistry 76:387-417.
2. Nilius, B., G. Owsianik, T. Voets, and J. A. Peters. 2007. Transient receptor potential cation channels in disease. Physiol. Rev. 87:165-217.
3. Cao, E., M. Liao, Y. Cheng, and D. Julius. 2013. TRPV1 structures in distinct conformations reveal activation mechanisms. Nature 504:113-118.
4. Zubcevic, L., M. A. Herzik Jr, B. C. Chung, Z. Liu, G. C. Lander, and S.-Y. Lee. 2016. Cryo-electron microscopy structure of the TRPV2 ion channel. Nature structural & molecular biology.
5. Doyle, D. A., J. M. Cabral, R. A. Pfuetzner, A. Kuo, J. M. Gulbis, S. L. Cohen, B. T. Cahit, and R. MacKinnon. 1998. The structure of the potassium channel: molecular basis of K^+ conduction and selectivity. Science 280:69-77.
6. Payandeh, J., T. Scheuer, N. Zheng, and W. A. Catterall. 2011. The crystal structure of a voltage-gated sodium channel. Nature 475:353-358.
7. Owsianik, G., K. Talavera, T. Voets, and B. Nilius. 2006. Permeation and Selectivity of TRP Channels. Annual Review of Physiology 68:685-717.

8. Caterina, M. J., M. A. Schumacher, M. Tominaga, T. A. Rosen, J. D. Levine, and D. Julius. 1997. The capsaicin receptor: a heat-activated ion channel in the pain pathway. Nature 389:816-824.
9. Roux, B., S. Berneche, B. Egwolf, B. Lev, S. Y. Noskov, C. N. Rowley, and H. Yu. 2011. Ion selectivity in channels and transporters. J Gen Physiol 137:415-426.
10. Maffeo, C., S. Bhattacharya, J. Yoo, D. Wells, and A. Aksimentiev. 2012. Modeling and Simulation of Ion Channels. Chemical Reviews 112:6250-6284.
11. Furini, S., and C. Domene. 2013. K(+) and Na(+) conduction in selective and nonselective ion channels via molecular dynamics simulations. Biophysical journal 105:1737-1745.
12. Darre, L., S. Furini, and C. Domene. 2015. Permeation and dynamics of an open-activated TRPV1 channel. Journal of Molecular Biology 427:537-549.
13. Laio, A., and M. Parrinello. 2002. Escaping free-energy minima. Proceedings of the National Academy of Sciences 99:12562-12566.
14. Laio, A., A. Rodriguez-Fortea, F. L. Gervasio, M. Ceccarelli, and M. Parrinello. 2005. Assessing the Accuracy of Metadynamics†. The Journal of Physical Chemistry B 109:6714-6721.
15. Torrie, G. M., and J. P. Valleau. 1977. Nonphysical sampling distributions in Monte Carlo free-energy estimation: Umbrella sampling. Journal of Computational Physics 23:187-199.
16. Darve, E., and A. Pohorille. 2001. Calculating free energies using average force. The Journal of Chemical Physics 115.
17. Domene, C., S. Furini, L. J. Michael, K. A. Gary, and M. H. Jo. 2009. Examining Ion Channel Properties Using Free-Energy Methods. In Methods in Enzymology. Academic Press. 155-177.
18. Piana, S., and A. Laio. 2007. A bias-exchange approach to protein folding. J Phys Chem B 111:4553-4559.
19. Berendsen, H. J. C., D. van der Spoel, and R. van Drunen. 1995. GROMACS: A message-passing parallel molecular dynamics implementation. Computer Physics Communications 91:43-56.
20. Phillips, J. C., R. Braun, W. Wang, J. Gumbart, E. Tajkhorshid, E. Villa, C. Chipot, R. D. Skeel, L. Kalé, and K. Schulten. 2005. Scalable molecular dynamics with NAMD. Journal of Computational Chemistry 26:1781-1802.
21. Domene, C., P. Barbini, and S. Furini. 2015. Bias-exchange metadynamics simulations: An efficient strategy for the analysis of conduction and selectivity in ion channels. Journal of Chemical Theory and Computation 11:1896-1906.
22. Hess, B., C. Kutzner, D. van der Spoel, and E. Lindahl. 2008. GROMACS 4: Algorithms for Highly Efficient, Load-Balanced, and Scalable Molecular Simulation. Journal of Chemical Theory and Computation 4:435-447.
23. Brooks, B., C. Brooks, A. MacKerell, L. Nilsson, R. Petrella, B. Roux, Y. Won, G. Archontis, C. Bartels, and S. Boresch. 2009. CHARMM: the biomolecular simulation program. Journal of computational chemistry 30:1545-1614.
24. Buck, M., S. Bouguet-Bonnet, R. Pastor, and A. MacKerell Jr. 2006. Importance of the CMAP correction to the CHARMM22 protein force field: dynamics of hen lysozyme. Biophysical Journal 90:L36-L38.

25. Jorgensen, W. L., J. Chandrasekhar, J. D. Madura, R. W. Impey, and M. L. Klein. 1983. Comparison of simple potential functions for simulating liquid water. The Journal of Chemical Physics 79.
26. Beglov, D., and B. Roux. 1994. Finite representation of an infinite bulk system: Solvent boundary potential for computer simulations. The Journal of Chemical Physics 100:9050-9063.
27. Bussi, G., D. Donadio, and M. Parrinello. 2007. Canonical sampling through velocity rescaling. The Journal of Chemical Physics 126:014101.
28. Parrinello, M., and A. Rahman. 1981. Polymorphic transitions in single crystals: A new molecular dynamics method. Journal of Applied Physics 52:7182-7190.
29. Darden, T., D. York, and L. Pedersen. 1993. Particle mesh Ewald: An N· log(N) method for Ewald sums in large systems. The Journal of Chemical Physics 98:10089-10092.
30. Hess, B. 2008. P-LINCS: A Parallel Linear Constraint Solver for Molecular Simulation. Journal of Chemical Theory and Computation 4:116-122.
31. Jo, S., T. Kim, V. G. Iyer, and W. Im. 2008. CHARMM-GUI: A web-based graphical user interface for CHARMM. Journal of Computational Chemistry 29:1859-1865.
32. Bonomi, M., D. Branduardi, G. Bussi, C. Camilloni, D. Provasi, P. Raiteri, D. Donadio, F. Marinelli, F. Pietrucci, R. A. Broglia, and M. Parrinello. 2009. PLUMED: A portable plugin for free-energy calculations with molecular dynamics. Computer Physics Communications 180:1961-1972.
33. Tribello, G. A., M. Bonomi, D. Branduardi, C. Camilloni, and G. Bussi. 2014. PLUMED 2: New feathers for an old bird. Computer Physics Communications 185:604-613.
34. Berneche, S., and B. Roux. 2001. Energetics of ion conduction through the K+ channel. Nature 414:73-77.
35. Furini, S., and C. Domene. 2012. Nonselective conduction in a mutated NaK channel with three cation-binding sites. Biophysical Journal 103:2106-2114.
36. Corry, B., and M. Thomas. 2012. Mechanism of ion permeation and selectivity in a voltage gated sodium channel. J Am Chem Soc 134:1840-1846.
37. Roux, B., and R. MacKinnon. 1999. The cavity and pore helices in the KcsA K^+ channel: electrostatic stabilization of monovalent cations. Science 285:100-102.
38. Liao, M., E. Cao, D. Julius, and Y. Cheng. 2013. Structure of the TRPV1 ion channel determined by electron cryo-microscopy. Nature 504:107-112.
39. Shelley, C., and K. L. Magleby. 2008. Linking exponential components to kinetic states in Markov models for single-channel gating. The Journal of general physiology 132:295-312.
40. Furini, S., F. Zerbetto, and S. Cavalcanti. 2007. Role of the intracellular cavity in potassium channel conductivity. The Journal of Physical Chemistry B 111:13993-14000.
41. Jogini, V., and B. Roux. 2005. Electrostatics of the intracellular vestibule of K+ channels. Journal of Molecular Biology 354:272-288.
42. Domene, C., S. Vemparala, S. Furini, K. Sharp, and M. L. Klein. 2008. The role of conformation in ion permeation in a K+ channel. Journal of the American Chemical Society 130:3389-3398.

43. Aqvist, J., and V. Luzhkov. 2000. Ion permeation mechanism of the potassium channel. Nature 404:881-884.
44. Furini, S., and C. Domene. 2009. Atypical mechanism of conduction in potassium channels. Proceedings of the National Academy of Sciences of the United States of America 106:16074-16077.
45. Stock, L., L. Delemotte, V. Carnevale, W. Treptow, and M. L. Klein. 2013. Conduction in a biological sodium selective channel. J Phys Chem B 117:3782-3789.
46. Furini, S., and C. Domene. 2012. On conduction in a bacterial sodium channel. PLOS Computational Biology 8:e1002476.
47. Berneche, S., and B. Roux. 2004. A gate in the selectivity filter of potassium channels. Biophysical Journal 86:9A-9A.
48. Domene, C., and S. Furini. 2009. Dynamics, Energetics, and Selectivity of the Low-K+ KcsA Channel Structure. Journal of Molecular Biology 389:637-645.
49. Furini, S., and C. Domene. 2011. Gating at the selectivity filter of ion channels that conduct Na+ and K+ ions. Biophysical Journal 101:1623-1631.
50. Chakrabarti, N., C. Ing, J. Payandeh, N. Zheng, W. A. Catterall, and R. Pomes. 2013. Catalysis of Na+ permeation in the bacterial sodium channel NaVAb. Proc Natl Acad Sci U S A 110:11331-11336.
51. Darré, L., and C. Domene. 2015. Binding of Capsaicin to the TRPV1 Ion Channel. Molecular Pharmaceutics.